Proceedings of the International Symposium on Engineering Lessons Learned from
the 2011 Great East Japan Earthquake, March 1-4, 2012, Tokyo, Japan

STRONG GROUND MOTION FROM THE 2010 Mw 8.8 MAULE CHILE EARTHQUAKE AND ATTENUATION RELATIONS FOR CHILEAN SUBDUCTION ZONE INTERFACE EARTHQUAKES

Rubén BOROSCHEK[1] and Víctor CONTRERAS[2]

[1] Associate Professor, Department of Civil Engineering, University of Chile, Santiago, Chile, rborosch@ing.uchile.cl
[2] Research Assistant, Department of Civil Engineering, University of Chile, Santiago, Chile, vicontre@ing.uchile.cl

ABSTRACT: The Mw 8.8 Maule Chile earthquake is one of the largest magnitude events to have produced strong motion recordings world-wide. In this paper we describe attributes of the recording stations, the data processing procedures and ground motion intensity measures computed from the records. We then compare spectral accelerations to predictions from GMPEs. Finally we present preliminary attenuation relations for horizontal spectral accelerations developed using a database of Chilean accelerograms recorded during interface earthquakes occurred between 1985 and 2010.

Key Words: Maule Chile earthquake, strong ground motion, attenuation, subduction zone, ground motion prediction

INTRODUCTION

The Mw 8.8 Chile earthquake occurred on February 27, 2010 in the south central Chilean region of Maule. This earthquake is associated with the subduction process of the Nazca plate beneath the South American plate, and it is one of the largest magnitude events to have produced strong motion recordings world-wide. There were around 30 relevant strong motion recordings from currently accessible arrays, over a rupture distance range of 30 to 700 km. These recordings come from the University of Chile research arrays.

In this paper we describe attributes of the recording stations, the data processing procedures, and ground motion intensity measures computed from the records. We then compare spectral accelerations to predictions from GMPEs. Existing well known GMPE for interface subduction events captures well the distance scaling and dispersion of the data, but under-predicts the overall ground motion level.

Finally we present attenuation formulas for horizontal Peak Ground Accelerations (PGA) and horizontal Spectral Accelerations (SA) obtained using a database of Chilean seismic records. The database used contains accelerograms recorded during interface earthquakes occurred between 1985 and 2010, including the accelerograms from the 2010 Mw 8.8 Maule Chile earthquake.

STRONG GROUND MOTION FROM THE 2010 Mw 8.8 MAULE CHILE EARTHQUAKE

The University of Chile (UCh) has maintained strong motion arrays in operation since the mid-1960, controlled by the National Accelerograph Network at the Department of Civil Engineering (RENADIC) and the Seismological Service at the Department of Geophysics (GUC). Most of the instruments are analogue accelerometers (SMA-1 or similar) located inside one story buildings. The Mw 8.8 Chile earthquake was recorded by the UCh strong motion arrays. Table 1 indicates location of the recording stations, orientation of the instruments and geological and geotechnical conditions.

Data processing procedure

The procedure used in record processing is similar to techniques described in the literature for high-cut filtering (Akkar et al. 2011) and for low-cut filtering (Akkar and Bommer 2006 and Paolucci et al. 2008). Recordings were digitized and processed in order to preserving high and low frequency signal to the extent possible. The Fourier Amplitude Spectrum (FAS) was inspected in log-log space to identify the maximum usable frequency (f_{max}) and to preliminarily estimate the low-cut filter corner (f_{min}). Typically, f_{max} was taken as 90 Hz for a Nyquist frequency of 100 Hz and 40 Hz for a Nyquist frequency of 50 Hz. An iterative process was performed to select the final value of f_{min}, in which the value was varied up and down and the integrated displacement histories and displacement response spectra were inspected. This process is illustrated in Fig. 1 for the VINA record. We seek the lowest value of f_{min} that preserves a natural appearance to the record in the time domain without obvious drift from low frequency noise. For the VINA record (NS component), f_{min} was selected as 0.03 Hz. Filtering was applied in the time domain using an acausal fourth order Butterworth filter. Finally, pseudo acceleration response spectra at 5% damping were calculated for a period band ending slightly short of 1/fmin. More details about record processing can be found in Boroschek et al. 2012.

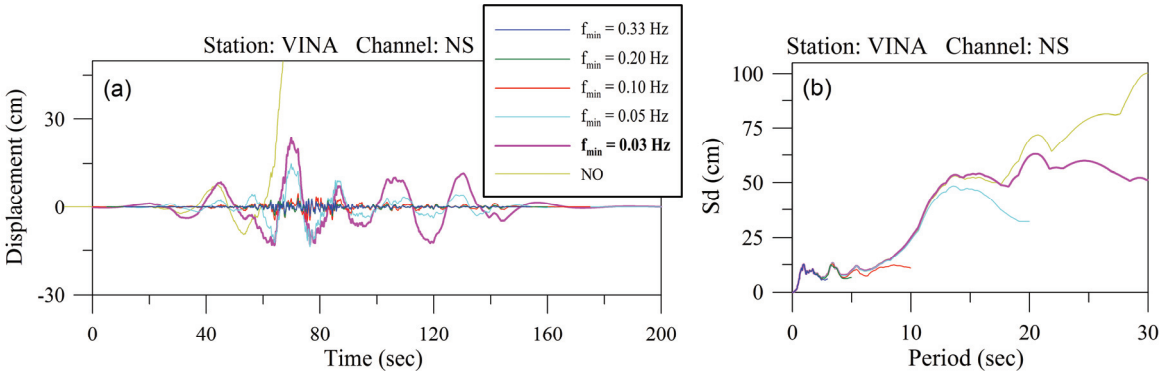

Fig. 1 Sensitivity of integrated displacements and displacement response spectra to different low-cut filter corners. The case indicated with 'NO' corresponds to direct integration of the VINA record.

Ground motion intensity measures of selected recordings

Finite fault models of the earthquake rupture have been generated by USGS 2010 and Delouis et al. 2010 (DEA) based on different data sources. The rupture plane used for distance calculation is trimmed from the DEA fault plane to envelope the high-slip region (530x150 km).

The closest instruments to the fault plane are in Concepción city: CCSP (relatively firm soil) and CONC (relatively soft soil) with rupture distances of 34-35 km. In Fig. 2(a) we present geometric mean spectra of these records. The relatively firm soil conditions at CCSP produced large spectral peaks above 2g at short periods (~0.2 s), while the softer conditions at CONC produced much lower short period spectral accelerations and a pronounced spectral peak from 1.5-2.2 s. The CONT station (soft soil) has much higher spectral ordinates over a broad period range (0.2 to 1.5 s), which may be a site effect that is much more broadly banded than that at CONC.

Table 1 Ground motion stations that recorded the 2010 Mw 8.8 Chile earthquake (adapted from Boroschek et al. 2012)

Station			Location		Orientation				Geological and geotechnical information available	
#	Code	Name	Lat (S)	Long (W)	Channels			Horizontal Azimuth	Surface geology[a]	V_{S30}[b]
1	COPI	COPIAPÓ-Hospital [RENADIC]	27.374	70.322	NS	EW	V	0	Clay with lenses of sand & gravel[1]	-
2	VALLE	VALLENAR-Liceo Santa Marta [RENADIC]	28.576	70.755	NS	EW	V	0	Continental sediments[2]*	-
3	PAP	PAPUDO [RENADIC]	32.507	71.448	L	T	V	60	Granite[3]; Weathered rock[3]	517[1]
4	ROBL	CERRO EL ROBLE [GUC]	32.976	71.016	NS	EW	V	0	Intrusive rock[2]	-
5	OLMU	OLMUÉ-Casa Particular [GUC]	32.994	71.173	NS	EW	V	0	Alluvial deposit[2]	-
6	VINA	VIÑA DEL MAR-Centro [RENADIC]	33.025	71.553	NS	EW	V	0	Alluvium & sand[3]; Sand[3]	273[1]
7	VALU	VALPARAÍSO-UTFSM [RENADIC]	33.035	71.596	L	T	V	180	Volcanic rock[3]; Rock[3]	1421[1]
8	MAR	VIÑA DEL MAR-Puente Marga Marga [RENADIC]	33.048	71.510	NS	EW	V	0	Silty sand with poorly graded gravel[4]	280[2]
9	VAL	VALPARAÍSO-Almendral [RENADIC]	33.048	71.604	L	T	V	310	Fill[3]; Soil[3]; Artificial fill[3]	360[1]
10	CASB	CASABLANCA-Teatro Municipal [GUC]	33.321	71.411	L	T	V	0	Poorly graded sand & clay[5]	~340[3]
11	LCON	LAS CONDES-Cerro Calán [GUC]	33.396	70.537	NS	EW	V	0	Gravel[6]	-
12	SLUC	SANTIAGO-Cerro Santa Lucía [GUC]	33.441	70.643	NS	EW	V	0	Intrusive rock[6]	-
13	LRNA	LA REINA-Colegio Las Américas [GUC]	33.452	70.531	NS	EW	V	0	Alluvium & gravel[7]	-
14	SANT	SANTIAGO-Conjunto Villa Andalucía [RENADIC]	33.467	70.652	L	T	V	270	Gravel[7]	-
15	HTIS	PEÑALOLÉN-Hospital Luis Tisné [RENADIC]	33.501	70.579	NS	EW	V	0	Clay & Gravel[5]	~452[3]
16	CRMA	MAIPÚ-Centro de Referencia de Salud [RENADIC]	33.509	70.772	NS	EW	V	0	Poorly graded gravel & pumicite[5]	~450[3]
17	MET	LA FLORIDA-Metro Línea 5 Estación Mirador [RENADIC]	33.514	70.606	NS	EW	V	0	Gravel[8]	~685[4]
18	ANTU	LA PINTANA-Antumapu [GUC]	33.569	70.634	NS	EW	V	0	Gravel[7]	-
19	HSOR	PUENTE ALTO-Hospital Sótero del Río [RENADIC]	33.577	70.581	NS	EW	V	0	Gravel & alluvium[8]	-
20	LLO	LLOLLEO [RENADIC]	33.616	71.611	L	T	V	340	Sandstone & volcanic rock[3]; Dense sand[3]	305[1]
21	SNJM	SAN JOSÉ DE MAIPO-Municipalidad [GUC]	33.641	70.354	NS	EW	V	0	Gravel[9]	-
22	MELP	MELIPILLA-Compañía de Bomberos [GUC]	33.687	71.214	L	T	V	0	Gravel[5]	~705[3]
23	MAT	MATANZAS-Escuela Carlos Ibáñez del Campo [RENADIC]	33.960	71.873	L	T	V	0	Sand[2]*	~400[3]
24	HUAL	HUALAÑÉ-Hospital [RENADIC]	34.977	71.805	L	T	V	0	Alluvium[3]; Dense Gravel[3]	527[1]
25	CURI	CURICÓ-Hospital [RENADIC]	34.990	71.236	NS	EW	V	150	Alluvial deposit[2]	~540[4]
26	CONT	CONSTITUCIÓN-Hospital [RENADIC]	35.340	72.406	L	T	V	0	Silt[10]	~340[3]
27	TAL	TALCA-Colegio Integrado San Pío X [RENADIC]	35.430	71.665	L	T	V	0	Alluvium[3]; Dense Gravel[3]	~640[3]
28	CONC	CONCEPCIÓN-Colegio Inmaculada Concepción [REN.]	36.828	73.048	L	T	V	60	Silty sand[11]	230[5]
29	CCSP	CONCEPCIÓN-Colegio San Pedro de la Paz [GUC]	36.844	73.109	NS	EW	V	0	Clay & gravel lying on metamorphic rock[5]	~395[3]
30	ANGO	ANGOL-Hospital [RENADIC]	37.795	72.706	NS	EW	V	0	Silt, clay & tuff[5]	~325[3]
31	VALD	VALDIVIA-Hospital [RENADIC]	39.831	73.239	NS	EW	V	0	Silty clay[2]*	-

a Description of the surface geology based on the following references: [1] Ruz, 2011; [2] Geologic map of Chile SNGM, 2003; [3] Arango et al., 2010; [4] Daza, 2003; [5] University of Chile, 2012; [6] Siebert et al., 2005; [7] Leyton et al., 2010; [8] Ortigosa, 2011; [9] Álvarez, 2006; [10] Taiba, 2010; [11] Ramírez and Vivallos, 2009.

b Average shear-wave velocity over the top 30 m, in m/sec, based on the following references: [1] Arango et al., 2010; [2] Daza, 2003; [3] U. of Chile, 2012; [4] Kataoka, 2011; [5] Ortigosa, 2011. For calculation purposes, when V_S data were available at depths <30 m, the V_S value of the last layer was assumed constant to 30 m depth.

***** Data indicated with asterisk correspond to preliminary information, which are still under investigation.

Fig. 2(b) shows geometric mean spectra of records with R_{rup}~50 km. LLO and HUAL stations are located around the north part of the fault and, despite the geographic distance between them (about 150 km), present similar spectral shapes. ANGO station, located around the south part of the fault, presents spectra with high accelerations for short periods and a large peak close to 3.5g at 0.2 s. Fig. 2(c) shows geometric mean spectra of seven records from the Santiago region. We observed similar spectral shapes with spectral peaks over a period range of 0.15 to 0.5 s. An exception is the CRMA station which presents higher short period spectral accelerations (by a factor of 2 compared with other records) and a spectral peak of 2g at 0.5 s. Fig. 2(d) shows geometric mean spectra from the Valparaíso and Viña del Mar region, where four stations are located very close to each other with rupture distances from 95-99 km. Data is plotted for stations VALU (rock) and three soil stations VINA, MAR, and VAL (soft soil). Site amplification is evident at the soil sites with apparent site periods of 0.5-1.0 s.

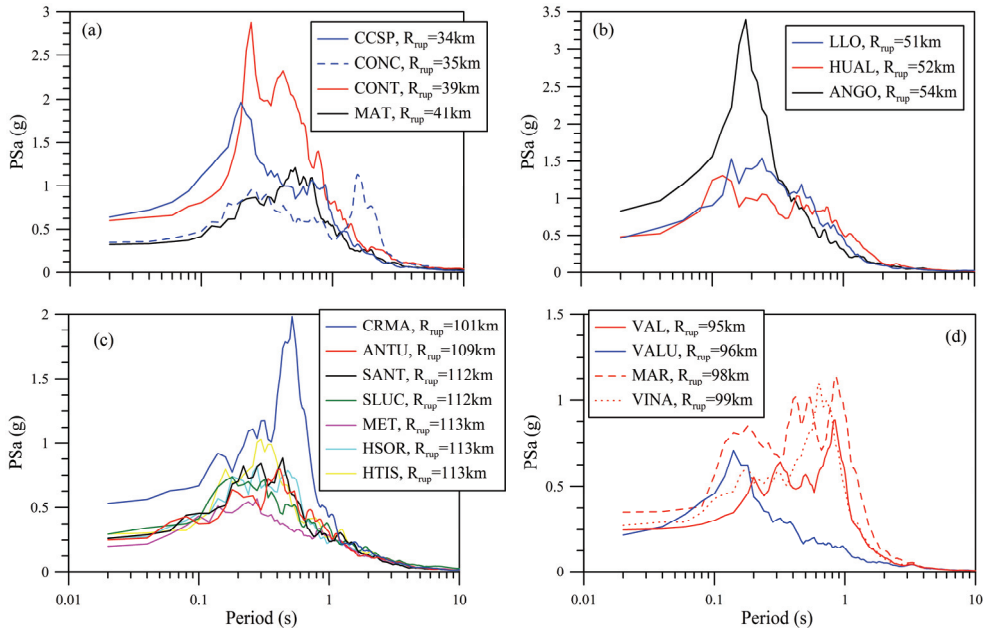

Fig. 2 Geometric mean spectra of some representative records

In Table 2 we present, for the closest sites to the fault, the intensity measures of: PGA, PGV, PGD and 5% damped PSa at 0.1, 0.2, 1.0, 2.0 and 3.0 s for the two horizontal components of recordings. The maximum PGA was 0.93g at station ANGO, the maximum PGV was 67 cm/s at station CONT and the maximum PGD was 40 cm at station SLUC. We also include in Table 2 Arias Intensity, Significant Duration (defined from the 5-95% time interval on a normalized Arias intensity plotted v/s time) and Central Frequency (Vanmarcke 1976). There is a strong motion record at Cauquenes that was saturated with a clip value of 1g. Additional studies are underway to derived reliable information.

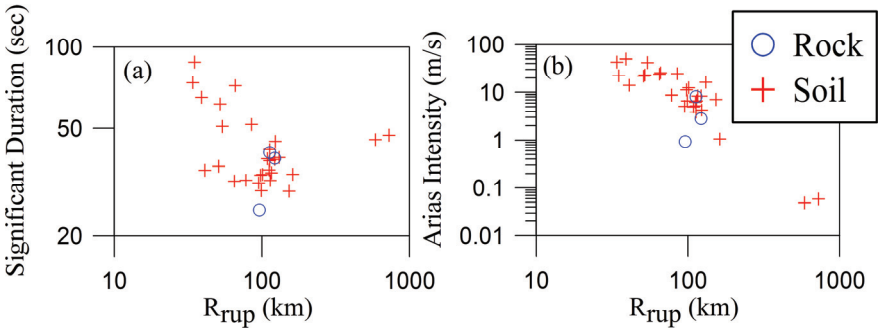

Fig. 3 (a) 5-95% Significant Duration and (b) Arias Intensity versus rupture distance

5-95% significant durations ranged from about 30-90 s, although perceptible durations were often much longer at 2-3 min. Fig. 3(a) shows variation of significant durations (maximum value of the two horizontal components is considered) with distance. It is observed a decreasing trend. Fig. 3(b) shows variation of Arias intensity (calculated as the sum of the Arias intensity of the three components).

Table 2 Ground motion intensity measures (derived from Boroschek et al., 2012)

Code Station (Rrup)	Channel	PGA (g)	PGV (cm/s)	PGD (cm)	5% damped PSa (g)					Arias Intensity (m/s)	Significant Duration (sec)	Central Freq. (Hz)
					0.1sec	0.2sec	1sec	2sec	3sec			
CCSP	NS	0.65	38	16	1.38	2.15	0.49	0.15	0.08	17.31	69.7	4.04
(34 km)	EW	0.61	44	15	0.91	1.79	0.81	0.30	0.08	14.26	73.8	4.16
CONC	L	0.40	67	21	0.61	1.05	0.39	1.13	0.18	8.79	80.6	2.13
(35 km)	T	0.28	50	16	0.39	0.67	0.35	0.51	0.14	5.72	**87.9**	2.54
CONT	L	0.55	44	11	0.70	1.68	0.57	0.34	0.13	19.85	59.8	2.97
(39 km)	T	0.63	**67**	16	0.93	1.83	1.14	0.25	0.17	**26.28**	65.2	2.82
MAT	L	0.34	42	9	0.41	0.85	0.72	0.35	0.15	7.10	34.0	2.29
(41 km)	T	0.30	28	7	0.42	0.77	0.41	0.18	0.09	4.55	35.0	2.89
LLO	L	0.32	26	4	0.85	1.08	0.32	0.08	0.05	5.00	36.2	4.36
(51 km)	T	0.57	31	5	1.03	1.82	0.66	0.11	0.06	10.26	32.0	4.16
HUAL	L	0.39	39	5	1.03	1.06	0.53	0.12	0.07	7.91	61.7	4.81
(52 km)	T	0.46	36	7	1.29	0.96	0.49	0.12	0.10	8.71	56.0	5.03
ANGO	NS	**0.93**	29	23	1.73	3.23	0.21	0.09	0.03	19.93	50.8	4.86
(54 km)	EW	0.68	40	34	1.49	2.37	0.46	0.16	0.07	17.54	49.8	4.76
MELP	L	0.57	24	6	1.11	1.90	0.17	0.09	0.07	8.99	31.9	6.96
(65 km)	T	0.77	42	12	1.29	1.60	0.60	0.11	0.09	12.69	31.8	5.97
TAL	L	0.48	28	4	0.77	1.22	0.31	0.13	0.05	11.61	69.9	5.14
(66 km)	T	0.42	34	7	1.01	1.79	0.38	0.19	0.08	11.06	71.9	5.14
CASB	L	0.29	33	7	0.37	0.56	0.28	0.06	0.03	3.68	32.2	2.89
(78 km)	T	0.33	27	17	0.49	0.71	0.51	0.07	0.04	3.80	30.1	2.97
CURI	NS	0.47	31	19	1.39	1.46	0.43	0.16	0.09	10.71	50.2	5.57
(85 km)	EW	0.41	37	29	1.08	1.11	0.41	0.17	0.07	11.06	51.7	4.68
VAL	L	0.22	29	5	0.28	0.45	0.68	0.10	0.04	2.30	31.4	1.92
(95 km)	T	0.27	22	4	0.33	0.66	0.49	0.08	0.04	2.04	27.3	2.44
VALU	L	0.14	7	2	0.35	0.30	0.13	0.04	0.04	0.28	25.0	5.13
(96 km)	T	0.31	16	3	0.60	0.72	0.15	0.07	0.04	0.50	21.9	4.62
MAR	NS	0.35	39	18	0.61	0.79	0.75	0.09	0.04	4.45	30.5	3.01
(98 km)	EW	0.34	46	12	0.52	0.80	1.12	0.17	0.06	4.73	33.6	3.03
VINA	NS	0.22	24	24	0.31	0.49	0.50	0.08	0.04	2.07	29.4	2.26
(99 km)	EW	0.33	35	21	0.58	0.60	0.46	0.07	0.06	3.84	24.6	1.85
CRMA	NS	0.56	47	15	0.61	0.96	0.38	0.12	0.07	5.77	32.1	2.60
(101 km)	EW	0.48	39	24	0.70	0.84	0.48	0.23	0.11	4.93	33.8	2.84
SLUC	NS	0.24	25	39	0.39	0.94	0.20	0.15	0.06	2.80	40.7	4.96
(113 km)	EW	0.34	44	**40**	0.44	0.47	0.63	0.23	0.14	2.80	37.8	3.64

Comparisons of spectral accelerations to predictions from GMPEs

We briefly compare in this section spectral accelerations to estimations from ground motion prediction equations (GMPEs), examining primarily the ground motion level and the distance attenuation of the Maule data. Relatively recent GMPEs for interface subduction zone earthquakes were developed by Atkinson and Boore 2003, 2008 and Zhao et al. 2006, which we referred to subsequently as AB03 and ZEA06. The AB03 interface model was derived exclusively from subduction zone interface earthquakes. In contrast, the ZEA06 model constrains near fault ground motions from crustal and slab earthquakes. Fig. 4 shows geometric mean PGA, 0.2 s, 1.0 s and 2.0 s pseudo spectral accelerations (PSa) at 5% damping versus rupture distance. Also shown in Fig. 4 are medians for the AB03 and ZEA06 GMPEs, plotted for the C/D boundary by averaging predictions for the two site classes.

It is observed that the variation of Maule data with distance is consistent with the AB03 GMPE, which was developed specifically for interface subduction earthquakes, but the Maule data are under-predicted by the AB03. The ZEA06 GMPE has significantly faster distance attenuation rates than the AB03 model and over-predicts the attenuation rate of the Maule data.

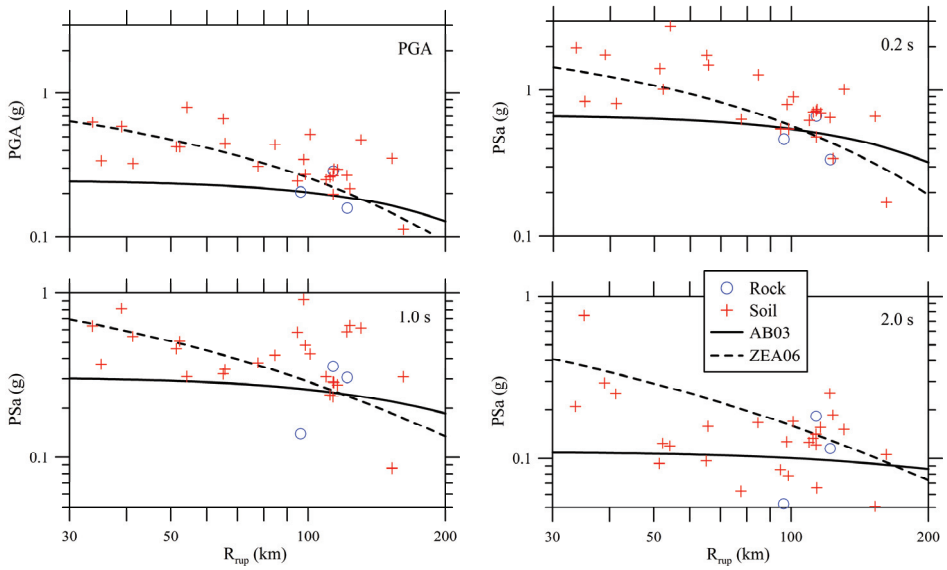

Fig. 4 Attenuation of PGA and spectral accelerations with distance and comparison to GMPEs

ATTENUATION RELATIONS FOR CHILEAN INTERFACE EARTHQUAKES

We present attenuation formulas for horizontal Peak Ground Accelerations (PGA) and horizontal Spectral Accelerations (SA) developed using a database of Chilean seismic records. Attenuation curves were estimated using the maximum likelihood regression method. The proposed formulas take into account differences in the soil type according to the Chilean code soil classification.

Strong Motion Database

The database used contains accelerograms recorded in Chilean territory during interface (thrust-faulting) earthquakes occurred between 1985 and 2010, including the accelerograms from the 2010 Mw 8.8 Maule Chile earthquake. The database was generated from public accelerographic data and accelerograms recorded by the UCh through the RENADIC and the Seismological Service (GUC). We used a subset of the overall database compiled considering only the interface events with magnitude Mw $\geq$ 6.5. The resulting subset consists in 117 accelerograms from 13 interface earthquakes recorded at 79 stations, located at distances between 30 and 600 km.

The earthquakes used in this study, listed in Table 3, correspond to 9 main events and 4 aftershocks with large magnitudes. Moment magnitude (Mw) was used, which was obtained from a search of the Harvard Centroid Moment Tensor (CMT). The date, time, location of the epicenters (Lat, Long) and focal depth (H) were taken from the Seismologic Service of the UCh. The epicenters of earthquakes and location of the recording stations are shown in Fig. 5 (in this Figure the earthquakes are listed as indicated in Table 3). Despite the small dataset, this is an initial attempt to capture the general behavior of GMPE at different SA periods for the country.

Due to the limited number of accelerograms used in this study, we decided to classify the sites of the recording stations only into two generic groups: Rock and Soil. Based on different type of geotechnical information we classify the sites according to the Chilean code soil classification, considering that the sites located on Rock comply with $V_{S30} \geq 900$ m/s (average shear wave velocity

over 30 m), or RQD ≥ 50% (Rock Quality Designation according to ASTM D 6032), or $q_u \geq 10$ MPa (Compressive Strength). In other cases we classify the sites as Soil.

Table 3 List of interface earthquakes used to develop attenuation relations

#	Date (dd-mm-yy)	UTC Time (hh:mm)	Mw	Lat. S	Long. W	H (km)	Number of Records	
							Rock	Soil
1	03-03-1985	22:46	7.9	-33.24	-71.85	33	5	22
2	03-03-1985[(a)]	23:38	7.3	-32.74	-71.21	33	1	2
3	09-04-1985[(a)]	01:56	7.1	-34.13	-71.62	38	1	9
4	30-07-1995	05:11	8.0	-23.57	-70.60	33	1	1
5	30-01-1998	12:16	7.0	-23.51	-69.83	44	1	0
6	23-06-2001	20:33	8.4	-16.26	-73.64	33	1	6
7	07-07-2001[(b)]	09:38	7.6	-17.40	-71.80	37	0	1
8	18-04-2002	16:08	6.6	-27.51	-70.09	53	1	0
9	20-06-2003	13:30	6.8	-30.65	-71.81	24	0	1
10	30-04-2006	21:40	6.5	-26.84	-71.15	18	0	2
11	14-11-2007	15:40	7.7	-22.69	-70.22	39	6	11
12	16-12-2007[(c)]	08:09	6.7	-22.95	-70.18	42	5	9
13	27-02-2010	06:34	8.8	-36.29	-73.24	30	3	28

(a) Aftershocks of the 03-03-1985 (22:46) earthquake. (b) Aftershock of the 23-06-2001 earthquake.
(c) Aftershock of the 14-11-2007 earthquake.

Focal mechanisms were obtained from published works and from the CMT solutions. This information was subsequently revised considering the proximity of the events to the subduction zone interface and the alignment of the mechanisms with the dip of the interface. The closest distance to the rupture surface (Rrup) is used as source to site distance. To estimate this parameter we modeled the earthquakes fault plane using the CMT solutions and the aftershocks distributions. For main events without a defined aftershock rupture area (events 5 and 8) and for aftershocks of the 03-03-1985 earthquake (events 2 and 3) we used hypocentral distance instead of Rrup. The magnitude-distance distribution of the database used is shown in the Fig. 6.

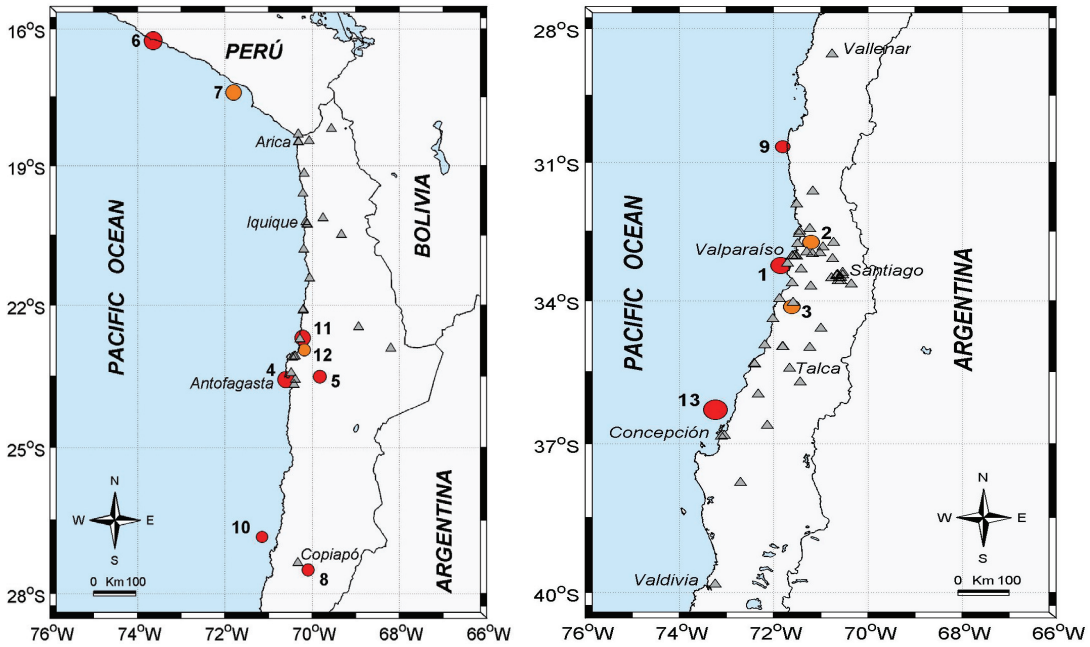

Fig. 5 Map of north and central Chile showing epicenters (listed circles) of earthquakes used in this study. Red circles correspond to main events and orange circles correspond to aftershocks. The circles size is proportional to the magnitudes. Grey triangles represent the strong motion stations.

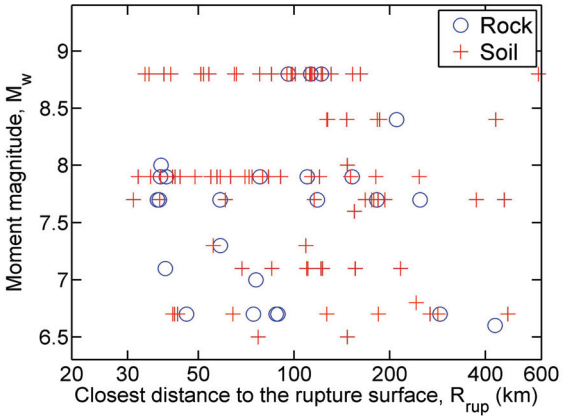

Fig. 6 Distribution of the data for interface earthquakes used in this study

Regression method and functional form

Regression of the database was performed using the one-stage maximum likelihood regression method. We used the following simple functional form:

$$\log_{10}(Y) = C_1 + C_2 M_w + C_3 H + C_4 R - g \log_{10}(R) + C_5 Z \quad (1)$$

where Y is either Peak Ground Acceleration (PGA) or 5% damped Spectral Acceleration (SA). In both cases the geometric mean of two horizontal components in units of g was used. M_W is the moment magnitude, H is the focal depth in kilometers, $R = \sqrt{R_{rup}{}^2 + \Delta^2}$ with R_{rup} the closest distance to the rupture surface in kilometers and Δ a near-source saturation term, given by $\Delta = C_6 10^{C_7 M_w}$. $g = C_8 + C_9 M_w$ is the geometrical spreading coefficient. For Rock sites $Z = 0$ and for Soil sites $Z = 1$. Coefficients C_i, with $i = 1,...,9$, were determined by regression analysis.

The coefficients C_6 and C_7 (associated to the near-source saturation term) and the coefficients C_8 and C_9 (associated to the geometrical spreading coefficient) were calculated using an optimization algorithm that allowed minimize the mean of residuals for the PGA data with distances lesser than or equal to 80 km. This subset of the data, consisting in 47 recordings, was selected considering the distance range where the possible saturation occurs. These coefficients were fixed for all periods analyzed. The coefficients C_1, C_2, C_3, C_4 and C_5 were calculated using the one-stage maximum likelihood regression method for each period; therefore the values of these coefficients vary with the period.

Results of the regression

The regression coefficients obtained for all the periods analyzed are shown in the Table 4. As found in previous work, there is a weak depth effect given by the coefficient C_3, with deeper events causing larger accelerations. Inspection of the coefficients C_5 shows that Soil accelerations exceed Rock accelerations by a factor ranging from 1.6 to 2. Standard deviations of the residuals (σ) are in the range of 0.21 to 0.26. Fig. 7 shows 0.04 and 1.0 s predicted spectral accelerations versus rupture distance for different magnitudes and soil conditions. It is clearly observed the effect of the saturation term for large magnitudes and near to fault distances. In Fig. 8 we compare predicted and observed accelerations for PGA, 0.4, 1.0 and 2.0 s, considering an earthquake with Mw=8.8 and H=30 km. Predicted curves proposed in this study for Rock and Soil are plotted. Also AB03 and ZEA06 models are plotted for the C/D boundary by averaging predictions for the two site classes.

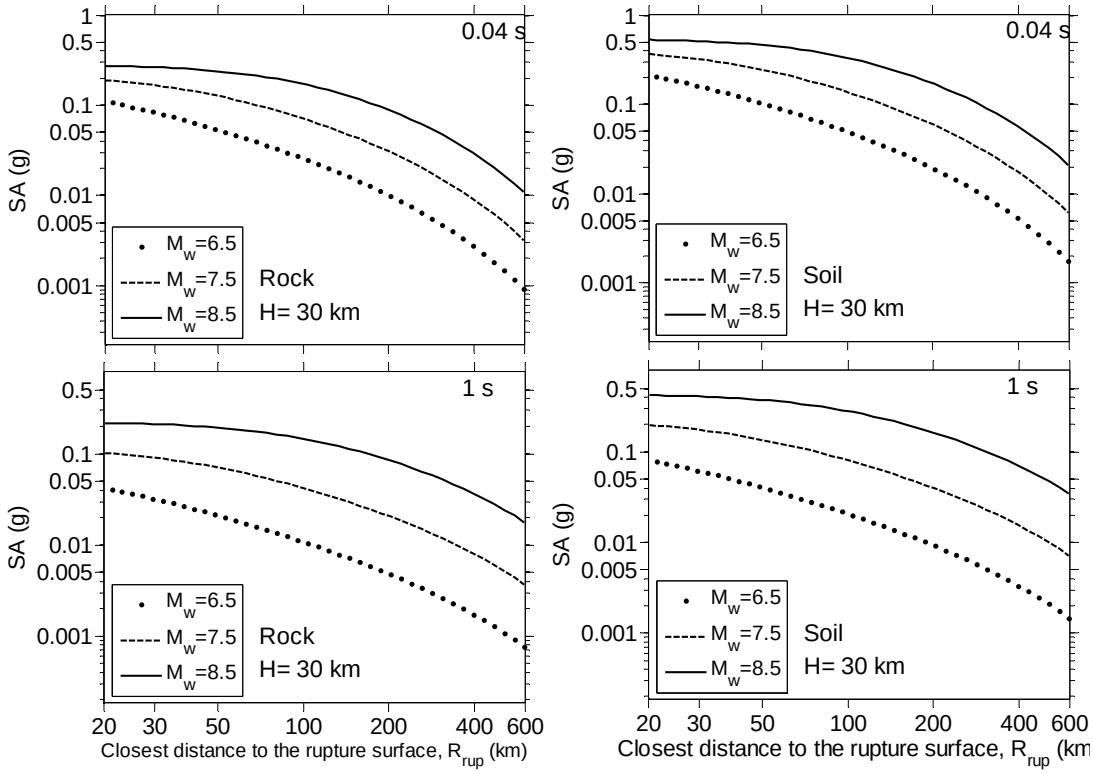

Fig. 7 Attenuation curves obtained plotted for different magnitudes

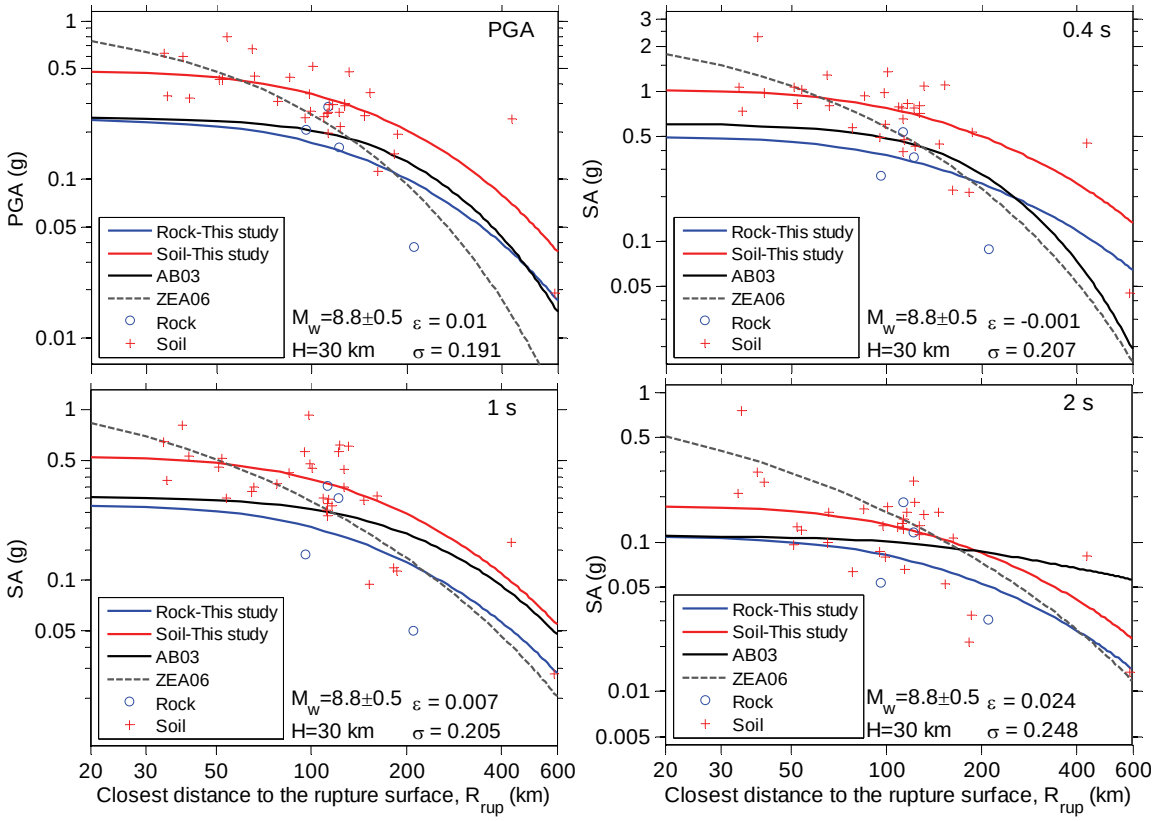

Fig. 8 Comparison between predicted and observed accelerations (Mw=8.8±0.5, H=30 km). The mean of residuals (ε) and the standard deviation of residuals (σ) for the data shown are indicated.

It is observed that the relations obtained present a good fit for the earthquake data plotted (Mw=8.8±0.5). AB03 GMPE under-predicts the acceleration level, but it is consistent with the variation of data with distance (excepting 2.0 s data). The ZEA06 GMPE over-predicts the attenuation rate.

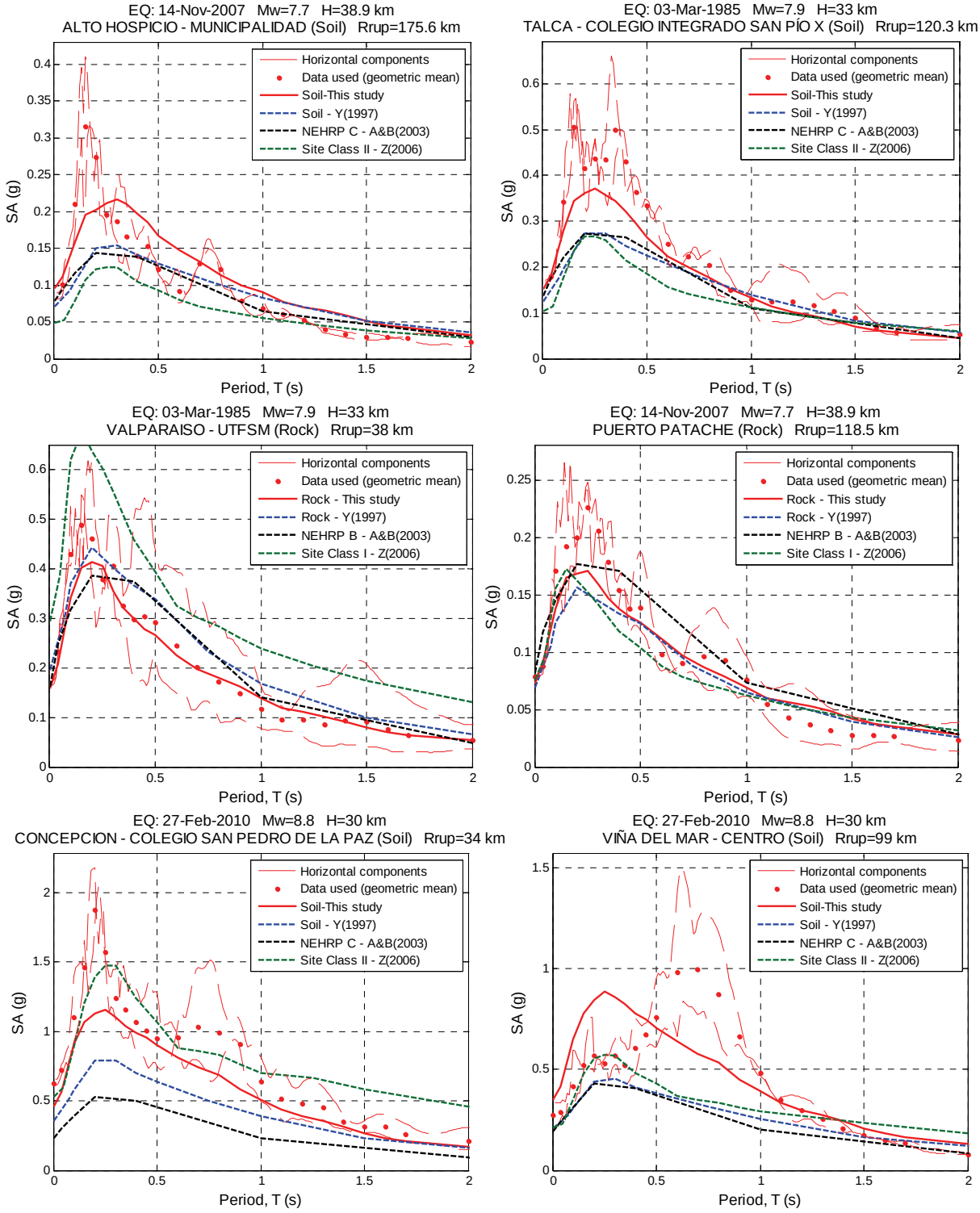

Fig. 9 Comparison of observed response spectra versus predicted response spectra

Fig. 9 shows a comparison of observed response spectra versus predicted response spectra for some representative records. The relations proposed in this study, generally result in higher accelerations than those estimated in other works, excepting the case of ZEA06 model for near to fault distances.

Table 4 Regression coefficients

Period (sec)	C_1	C_2	C_3	C_4	C_5	C_6	C_7	C_8	C_9	σ
PGA	-1.8559	0.2549	0.0111	-0.0013	0.3061	0.0734	0.3552	1.5149	-0.103	0.2137
0.04	-1.7342	0.2567	0.0111	-0.0016	0.2865	0.0734	0.3552	1.5149	-0.103	0.2311
0.10	-1.4240	0.2597	0.0081	-0.0019	0.2766	0.0734	0.3552	1.5149	-0.103	0.2557
0.20	-1.0028	0.2375	0.0023	-0.0014	0.2699	0.0734	0.3552	1.5149	-0.103	0.2469
0.30	-1.2836	0.2519	0.0044	-0.0009	0.2977	0.0734	0.3552	1.5149	-0.103	0.2434
0.40	-1.4161	0.2568	0.0049	-0.0008	0.3150	0.0734	0.3552	1.5149	-0.103	0.2414
0.50	-2.1228	0.3208	0.0094	-0.0008	0.2834	0.0734	0.3552	1.5149	-0.103	0.2272
0.60	-2.7134	0.3668	0.0141	-0.0008	0.2824	0.0734	0.3552	1.5149	-0.103	0.2174
0.70	-2.9001	0.3795	0.0152	-0.0009	0.2969	0.0734	0.3552	1.5149	-0.103	0.2221
0.80	-3.0909	0.4005	0.0147	-0.0009	0.2834	0.0734	0.3552	1.5149	-0.103	0.2279
0.90	-3.1439	0.3952	0.0163	-0.0010	0.2730	0.0734	0.3552	1.5149	-0.103	0.2260
1.00	-3.3352	0.4013	0.0186	-0.0010	0.2839	0.0734	0.3552	1.5149	-0.103	0.2351
1.10	-3.5092	0.4093	0.0202	-0.0011	0.2849	0.0734	0.3552	1.5149	-0.103	0.2379
1.20	-3.5599	0.4079	0.0211	-0.0011	0.2700	0.0734	0.3552	1.5149	-0.103	0.2374
1.30	-3.6365	0.4090	0.0218	-0.0010	0.2631	0.0734	0.3552	1.5149	-0.103	0.2429
1.40	-3.7061	0.4096	0.0225	-0.0010	0.2555	0.0734	0.3552	1.5149	-0.103	0.2425
1.50	-3.7750	0.4089	0.0228	-0.0010	0.2528	0.0734	0.3552	1.5149	-0.103	0.2459
2.00	-3.9051	0.4079	0.0215	-0.0008	0.2057	0.0734	0.3552	1.5149	-0.103	0.2592

CONCLUSIONS

The 2010 Mw 8.8 Maule Chile earthquake produced about 30 relevant strong motion recordings over a rupture distance range of 30 to 700 km. The strong motion data were processed using high- and low-cut filters designed to optimize the usable frequency range. Ground motion intensity measures were presented, including PGA, PGV, PGD, 5% damped pseudo spectral accelerations, 5-95% significant duration, Arias intensity and Central frequency. Significant durations for this earthquake generally ranged from about 30 to 90 s. Data from the Concepción and Viña del Mar areas exhibit site effects with respective site periods of about 1.5-2.2 s and 0.5-1.0 s. The variation of Maule data with distance is consistent with the AB03 GMPE, but the Maule data are under-predicted by the AB03 model. The ZEA06 GMPE over-predicts the attenuation rate of the Maule data.

Accelerograms database was generated from public accelerographic data and data recorded by the University of Chile. The earthquake database analyzed enabled a gross estimation of attenuation relations for Chilean interface earthquakes. These GMPEs could be useful to improve the seismic hazard assessment in Chile and others similar subduction zones. In particular, the relations obtained present a good fit for earthquakes with larger magnitudes, and the logarithmic standard deviations of the errors are in the range 0.21 to 0.26. The obtained curves indicate that the accelerations at stations located in Soil are higher than those estimated at stations located on Rock by a factor of up to 2. For the Chilean case, the horizontal accelerations are generally higher than those estimated in studies where records from different subduction zones around the world are mixed. This issue highlights the need to develop GMPEs for specific subduction zones.

ACKNOWLEDGMENTS

The financial and technical support of the Civil Engineering Department of University of Chile and the effort of Eng. Pedro Soto installing and maintaining the instruments are gratefully acknowledged.

REFERENCES

Akkar S. and Bommer J. J. (2006). “Influence of long-period filter cut-off on elastic spectral displacements”, *Earthquake Engineering & Structural Dynamics* 35, 1145–1165.

Akkar S., Kale Ö., Yenier E. and Bommer J. J. (2011). “The high-frequency limit of usable response spectral ordinates from filtered analogue and digital strong-motion accelerograms”, *Earthquake Engineering & Structural Dynamics* 40, 1387–1401.

Álvarez M. (2006). “Factibilidad de utilización de técnicas geofísicas en estudios de fenómenos de remoción en masa. Caso: deslizamiento de San José de Maipo”, Memoria para optar al título de geólogo, Facultad de Ciencias Físicas y Matemáticas, U. de Chile. Santiago, Chile (in Spanish).

Arango M. C., Strasser F. O., Bommer J. J., Boroschek R., Comte D. and Tavera H. (2010). “A strong-motion database from the Peru–Chile subduction zone”, *J. Seismology*, 15, 19-41.

Atkinson G. M. and Boore D. M. (2003). “Empirical Ground-Motion Relations for Subduction-Zone Earthquakes and Their Application to Cascadia and Other Regions”, *Bulletin of the Seismological Society of America*, Vol. 93, N° 4, pp. 1703-1729, August.

Atkinson G. M. and Boore D. M. (2008). “Erratum to Empirical Ground-Motion Relations for Subduction-Zone Earthquakes and Their Application to Cascadia and Other Regions”, *Bulletin of the Seismological Society of America*, Vol. 98, N° 5, pp. 2567-2569, October.

Boroschek R., Contreras V., Youp D. and Stewart J. (2012). “Strong Ground Motion Attributes of the 2010 Mw 8.8 Maule Chile Earthquake”, *Earthquake Spectra.* Accepted for publication.

Daza V. (2003). “Interacción sísmica suelo-estructura en el puente Marga-Marga”, Memoria para optar al título de ing. Civil, Fac. de Cs. Físicas y Matemáticas, U. de Chile. Santiago, Chile (in Spanish).

Delouis B., Nocquet J-M and Vallée M. (2010). “Slip distribution of the February 27, 2010 Mw=8.8 Maule Earthquake, central Chile, from static and high-rate GPS, InSAR, and broadband teleseismic data”, *Geophy. Res. Ltrs*, 37, L17305.

Kataoka S. (2011). “Microtremor exploration at seven strong motion stations in Chile”, *4th IASPEI/IAEE International Symposium: Effects of Surface Geology on Seismic Motion*, August 23-26, University of California Santa Barbara.

Leyton F., Sepúlveda S. A., Astroza M., Rebolledo S., González L., Ruiz S., Foncea C., Herrera M. and Lavado J. (2010). “Zonificación Sísmica de la Cuenca de Santiago, Chile”, *Congreso Chileno de Sismología e Ing. Antisísmica, X Jornadas*, 22-27 Mayo. Valdivia-Santiago, Chile (in Spanish).

Ortigosa P. (2011). Personal communication. PETRUS Consultores Geotécnicos, Santiago, Chile.

Paolucci R., Rovelli A., Faccioli E., Cauzzi C., Finazzi D., Vanini M., Di Alessandro C., Calderoni G. (2008). “On the reliability of long period spectral ordinates from digital accelerograms”, *Earthquake Engineering & Structural Dynamics* 37, 697–710.

Ramírez P. and Vivallos J. (2009). “Microzonificación sísmica de la ciudad de Concepción-Chile”, *XII Congreso Geológico Chileno*, 22-26 de Noviembre. Santiago, Chile (in Spanish).

Ruz M. (2011). Personal communication. Ruz & Vukasovic Ing. Asociados Ltda., Santiago, Chile.

Siebert E., Rebolledo S., Verdugo R., Campos J. (2005). “Respuesta sísmica y caracterización geológico-geotécnica de sitios donde están instaladas estaciones sismológicas en Santiago”, *Congr. Chileno de Sismología e Ing. Antisísmica, IX Jorns.*, 16-19 Nov. Concepción, Chile (in Spanish).

SNGM (2003). “1:1.000.000 geologic map of Chile”, Servicio Nacional de Geología y Minería, Chile.

Taiba O. (2010). Personal communication. Pilotes Terratest S.A., Santiago, Chile.

University of Chile (2012). Department of Civil Engineering. Santiago, Chile.

Vanmarcke E. (1976). “Structural Response to Earthquakes”, *Chapter 8 in Seismic Risk and Engineering Decisions*, Lomnitz C. and Rosemblueth E.

Youngs, R.R., S.-J. Chiou, W.J. Silva, and J.R. Humphrey (1997). “Strong ground motion attenuation relationships for subduction zone earthquakes”, *Seismol. Res. Let.* 68, N°1, pp. 58–73, Jan./Febr.

Zhao J. X., Zhang J., Asano A., Ohno Y., Oouchi T., Takahashi T., Ogawa H., Irikura K., Thio H. K., Somerville P. G., Fukushima Y. and Fukushima Y. (2006). “Attenuation relations of strong ground motion in Japan using site classification based on predominant period”, *Bull. Seis. Soc. Am.* 96 898-913.